Characterization of PM_{10} sources in the central Mediterranean

G. Calzolai[1,2,*], S. Nava[2], F. Lucarelli[1,2], M. Chiari[2], M. Giannoni[3,2], S. Becagli[3], R. Traversi[3], M. Marconi[3], D. Frosini[3], M. Severi[3], R. Udisti[3], A. di Sarra[4], G. Pace[4], D. Meloni[4], C. Bommarito[5], F. Monteleone[5], F. Anello[5], D. M. Sferlazzo[6]

[1]*Department of Physics and Astronomy, University of Florence, Via G. Sansone 1, 50019 Sesto Fiorentino (Florence), Italy*

[2]*National Institute for Nuclear Physics – Florence, Via G. Sansone 1, 50019 Sesto Fiorentino (Florence), Italy*

[3]*Department of Chemistry, University of Florence, Via della Lastruccia 3, 50019 Sesto Fiorentino (Florence), Italy*

[4]*ENEA Lab. for Earth Observations and Analyses, 0012, S. Maria di Galeria, Roma, Italy*

[5]*ENEA, Laboratory for Earth Observations and Analyses, 90141 Palermo, Italy*

[6]*ENEA, Laboratory for Earth Observations and Analyses, 92010 Lampedusa, Italy*

Abstract

The Mediterranean Basin atmosphere is influenced by both strong natural and anthropogenic aerosol emissions, and is also subject to important climatic forcings. Several programs have addressed the study of the Mediterranean basin; nevertheless important pieces of information are still missing. In this framework, PM_{10} samples were collected on a daily basis on the island of Lampedusa (35.5° N, 12.6° E, 45 m a.s.l.), which is far from continental pollution sources (the nearest coast, in Tunisia, is more than 100 km away). After mass gravimetric measurements, different portions of the samples were analyzed to determine the

---

[*] Corresponding author: Giulia Calzolai, Via Sansone 1, I-50019 Sesto Fiorentino (Firenze), Italy.
Tel ++39 055 4572273; fax ++39 055 4572641.
E-mail address: calzolai@fi.infn.it

ionic content by Ion Chromatography (IC), the soluble metals by Inductively Coupled Plasma Atomic Emission Spectrometry (ICP-AES), and the total (soluble + insoluble) elemental composition by Particle Induced X-ray Emission (PIXE). Data from years 2007 and 2008 are used in this study.

The Positive Matrix Factorization (PMF) model was applied to the 2-year long data set of PM_{10} mass concentration and chemical composition to assess the aerosol sources affecting the Central Mediterranean basin. Seven sources were resolved: sea-salt, mineral dust, biogenic emissions, primary particulate ship emissions, secondary sulphate, secondary nitrate, and combustion emissions. Source contributions to the total PM_{10} mass were estimated to be about 40% for sea-salt, around 25% for mineral dust, 10% each for secondary nitrate and secondary sulphate, and 5% each for primary particulate ship emissions, biogenic emissions, and combustion emissions. Large variations in absolute and relative contributions are found and appear to depend on the season and on transport episodes. In addition, the secondary sulphate due to ship emissions was estimated, and found to contribute by about one third to the total sulphate mass. Results for the sea-salt and mineral dust sources were compared with estimates of the same contributions obtained from independent approaches, leading to an estimate of the water content bound to the sea salt in the marine source.

Keywords: Mediterranean Basin, aerosol sources, PM_{10}, PMF, Central Mediterranean Sea.

1. Introduction

Atmospheric aerosols are estimated to have negative effects on human health and to play a relevant role in climate, also affecting the hydrological cycle (IPCC). In this context, the Mediterranean Basin is a complex area, due to the strong influences from both natural and anthropogenic emissions, to the peculiar meteorology of the basin, and to conditions (high solar irradiation, summer temperature, humidity) favouring secondary aerosol formation processes (Pey et al., 2009; Im et al., 2012). Information on the aerosol sources and properties in the Mediterranean area is essential for the determination of the impacts on the health of the population living in the countries facing the Basin (among the world's most populated areas) and on the climate of the area. This is particularly important because future climate projections by IPCC consider the Mediterranean among the regions most sensitive to climate change (IPCC).

Owing to its importance, Mediterranean atmospheric aerosol and meteorology have been intensively studied (e.g., Salvador et al., 2014; Pey et al., 2013; Pace et al., 2006; Kopanakis et al., 2012; Dayan et al., 1989) and several international programs have focused on the assessment of chemistry and climate and their interactions, nevertheless important pieces of information are still missing. For instance, the source contribution and the forcing of short-lived species (both of them highly space and time variable) remain uncertain, and are not well taken into account in climate simulation.

Without aiming at a thorough review of the published information, it is worthy to recall that PM_{10} concentration is observed to increase from North-Western to South-Eastern Mediterranean due to increasing contributions from both natural and anthropogenic sources (Pey et al., 2013); the Western and Eastern Mediterranean basins have been observed to be characterized by different atmospheric dynamical and chemical processes (e.g., neutralization of secondary aerosol (Querol et al., 2009)). The Mediterranean boundary layer has been observed to generally follow a clear annual behaviour, with minimum vertical extension during summer and maximum altitudes in winter (with an opposite trend with respect to the one commonly observed in continental areas) (Pey et al., 2009, Dayan et al., 1989; Pace et al., 2012); therefore, stagnation of pollutants is favoured in summer over the Mediterranean basin.

Most of the studies performed in the Mediterranean area are based on samplings carried out at coastal sites, with strong influences from the continental meteorology and from anthropogenic sources; thus, regional background and remote sites are essential for the study of natural sources and to obtain information on the Mediterranean basin (Querol et al., 2009; Pey et al., 2009; Koulouri et al., 2008; Pace et al., 2006). In this context, the island of Lampedusa represents an ideal site: in fact, Lampedusa's environment is poorly affected by anthropogenic pollution sources from local origin, due to its scarce population and industrialization, and from abroad, as it is more than 100 km far from the nearest coast. As discussed by (Henne et al., 2010), Lampedusa is one of the most remote sites with respect to air quality measurements among 34 measurement stations throughout Europe. In addition, Lampedusa is located in the Central Mediterranean Sea, in an area where few remote or background sampling sites exist, despite the crucial position: in fact, as previously mentioned, Western and Eastern Mediterranean Basin areas are known to be prone to different atmospheric dynamics and pollution conditions.

In this work, an investigation aimed at assessing the aerosol sources affecting the Central Mediterranean basin and at quantifying their contributions has been carried out. This study answers to one of the main scientific question of the ChArMEx (Chemistry-Aerosol Mediterranean Experiment) initiative. ChArMEx proposes to set up a coordinated experimental and modelling international effort based on most updated tools, for an assessment of the regional budgets of tropospheric trace species, of their trends, and of their impacts on air quality, marine biogeochemistry, and regional climate. The source apportionment here applied is based on the application of the Positive Matrix Factorization (PMF) model to a 2-year long data set of PM_{10} mass concentration and chemical composition of samples collected on the Lampedusa Island. It is worth to recall that information on aerosol sources and impact are among the data needed to constrain uncertainties in climate change models, and they are also important for local administrations and policy makers for the development of effective pollution abatement strategies. Studies on the source assessment/apportionment of aerosols, often focused on specific sources such as African dust or ship emissions, are available in literature for sites in the Western Mediterranean (e.g., Montseny (Cusack et al., 2013) and Palma de Mallorca (Pey et al., 2009) in Spain) and in the Eastern Mediterranean (e.g., the Greek islands of Crete (Koulouri et al., 2008, Hildebrandt et al., 2011) and Rhodes (Argyropoulos et al., 2012)). This work adds an important piece of information still missing in the Central Mediterranean area.

2. Materials and methods

2.1 Sampling site and instrumentation

As previously mentioned, sampling was performed on Lampedusa (Italy), a small island located in the Central Mediterranean, far from continental pollution sources (the nearest coast, in Tunisia, is more than 100 km away). More in detail, sampling was carried out on the plateau on the North-Eastern coast, at the Station for Climate Observations (35.5° N, 12.6° E, 45 m a.s.l., see Figure 1), maintained by ENEA (Italian Agency for New Technologies, Energy and Sustainable Economic Development), where continuous observations of greenhouse gases concentration (Artuso et al., 2009), total ozone (Gomez Amo et al., 2012), ultraviolet irradiance (Meloni et al., 2005), aerosol properties (Pace et al., 2005, 2006; Di

Iorio et al., 2009; Marconi et al., 2014) and other climatic parameters (Di Biagio et al., 2009; di Sarra et al., 2011) are routinely carried out.

Daily PM_{10} samples have been collected at this station since 2004, every third day up to 2006 (Becagli et al., 2012; Marconi et al., 2014), and every day since 2007. Particulate was sampled by a low volume sequential sampler (2.3 m^3/h) equipped with a PM_{10} inlet, on 47 mm diameter 2 μm nominal porosity Pall Gelman Teflon filters.

This paper focuses on the 2-years data set relative to the years 2007-2008, when PM_{10} was collected every day, accounting for a total of 562 samples (due to episodic technical failures, some short sampling interruptions occurred in the period).

Additional samplings of PM_{10} on quartz filters were performed in 2007, from 16 May to 15 August, using a low volume Tecora ECHO-PM sampler (2.3 m^3/h), with collection times ranging from 24 to 72h, for a total of 24 samples.

2.2 Analyses

The mass of the collected PM_{10} was obtained by gravimetric measurements of the Teflon filters before and after sampling. Before weighting, filters were conditioned for at least 24 hours in an environmentally controlled room (35-45% relative humidity, 25°C).

Afterwards, every Teflon filter was cut into three portions: a quarter was analyzed for the ionic content by Ion Chromatography (IC), a second quarter for soluble metals by Inductively Coupled Plasma Atomic Emission Spectrometer (ICP-AES); the remaining half filter was analyzed for the total (soluble + insoluble) elemental composition by Particle Induced X-ray Emission (PIXE).

More in detail, the quarter of Teflon filter devoted to ion chromatography was extracted in about 10 mL (accurately weighted) of ultra-pure water (MilliQ water, resistivity>18 MΩ) in ultrasonic bath for 15 min and analysed for the ionic content by using 3 Dionex ion chromatographs fed by an auto-sampler. Cations (Na^+, NH_4^+, K^+, Mg^{2+}, Ca^{2+}), inorganic anions (F^-, Cl^-, NO_3^-, SO_4^{2-}), and some organic anions (methanesulphonate – MSA, acetate, formate, glycolate, oxalate) were determined for each sample as reported in (Becagli et al. 2011). Detection limits (DLs) were in the range 0.08-0.16 ng/m^3 and reproducibility was better than 5% .

Another quarter was extracted in ultrasonic bath for 15 min with MilliQ water acidified at pH 1.5–2 with ultra-pure nitric acid obtained by sub-boiling distillation. This extract was used for the determination of the soluble part of selected metals (Al, As, Ba, Cd, Cr, Cu, Fe, Mn, Mo, Ni, Pb, V, Zn) with an Inductively Coupled Plasma Atomic Emission Spectrometer (ICP-AES, Varian 720-ES) equipped with an ultrasonic nebulizer (U5000 AT+, Cetac Technologies Inc.). The value of pH was chosen because it is the lowest value found in rainwater (Li and Aneja, 1992) and therefore it leads to the determination of the metal fraction more representative of the anthropogenic sources (Becagli et al., 2012; Traversi et al., 2014).

PIXE measurements on the remaining half Teflon filters were performed at the INFN-LABEC laboratory, equipped with a 3MV Tandetron accelerator, where research is focused in the fields of cultural heritage (Castelli et al., 2013; Fedi et al., 2013), material science, and atmospheric aerosols (Moreno et al., 2013, Calzolai et al., 2011). The PIXE technique is based on the detection and analysis of the X-rays emitted by the sample after excitation by an accelerated particle beam, and allows the quantification of $Z>10$ elements. Briefly, samples were bombarded by a 3.2 MeV proton beam ($i \sim 5$ nA, $t \sim 300$ s) using the set-up widely described elsewhere (Calzolai et al., 2006; Lucarelli et al., 2011); spectra were fitted using the Gupix software package (Campbell et al., 2010) and elemental concentrations were obtained via calibration relative to thin reference standards. Detection limits (DLs) are in the 1-20 ng/m^3 range. Uncertainties were determined by a sum of independent uncertainties on certified standard sample thickness (5%), peak areas (from 2 to 20% or higher when concentrations approach DLs) and sampling parameters (of the order of few percent). The concentrations of lighter elements (Na, Mg, Al and Si) were corrected for self-absorption effects, i.e. lower energy X-rays attenuation inside aerosol particles. Correction factors were estimated on the basis of PIGE (Particle Induced γ-ray Emission) measurements carried out for the quantification of Na (Calzolai et al., 2010), using an attenuation model for single spherical particles (Formenti et al., 2010); the uncertainty on the PIXE quantification of light elements also bears the uncertainty on these correction factors (of the order of few percent).

As regards the additional samplings carried out in May-August 2007, the 24 samples collected on quartz fibre filters were analyzed for total, elemental and organic carbon fractions (TC, EC and OC) by a Sunset thermo-optical transmittance analyser following a proxy of the IMPROVE protocol (He-580 in (Piazzalunga et al., 2011)).

2.3 PMF analysis

The Positive Matrix Factorization (PMF) is a receptor model allowing the determination of the chemical profiles of the aerosol sources affecting the receptor site and the estimation of their contributions to the aerosol load, using as input data the atmospheric concentrations of different chemical species.

Briefly, PMF is an advanced factor analysis technique (Paatero, 1997; Paatero and Hopke, 2003) that uses realistic error estimates to weigh data values and imposes non-negativity constraints in the computational process, which is based on a weighted least-squares approach. With more detail, PMF model may be written as $X=G \cdot F+E$, where X is the n x m matrix of the m measured chemical species in n samples and G and F are factor matrices to be determined: G is the n x p matrix of source contributions to the samples; F is the p x m matrix of factor composition (source profiles); E is the residual matrix.

Input data were handled according to (Polissar et al., 1998): measured data were weighted with their overall analytical uncertainty increased by one third of the detection limit (DL); data below the DL were substituted with a value corresponding to DL/2, and a DL*5/6 uncertainty was associated to them. Missing data were handled filling the gaps with the geometric mean value calculated over the days with data and associating to them a 400% uncertainty.

Mass concentration was put in the PMF analysis as an internal variable, with very high (400%) uncertainty (Norris et al., 2009), as it is suggested when portions of the mass (not directly correlated with the other input variables) are not measured/available: in our case, no data on the carbonaceous fraction is available for the whole considered period. As additional test, PMF was also run with normalization of G and F matrices by multilinear regression analysis on the PM_{10} gravimetric mass concentrations and gave comparable results for both contributions and profiles of the detected sources with respect to PMF runs performed with internal mass, thus assuring that mass data did not influence the profiles.

PMF was run with the algorithm PMF2 (Paatero, 1997) in the robust mode, in order to reduce the influence of outliers. Solutions with different numbers of factors were examined; rotational ambiguity was tested by analyzing multiple FPEAK rotations; several seeds were investigated and values of Q/Q_{exp} were examined (where Q is the weighted least-squares function to be minimized).

3. Results and discussion

3.1 PM_{10} concentration

The PM_{10} daily concentration is reported in figure 2: a great variability was observed, with values spanning one order of magnitude, as minima were found to be around 10 μg/m^3 and several episodes reached more than 100 μg/m^3.

The average PM_{10} concentration for the whole period (2007-2008) was 32 ± 17 μg/m^3 (median: 29 μg/m^3, 25th percentile 21 μg/m^3, 75th percentile 39 μg/m^3); no relevant difference was observed between the two years 2007 and 2008, with mean PM_{10} concentrations of 33 ± 15 μg/m^3 and 32 ± 19 μg/m^3, respectively. These values are similar to those measured in two different background/rural stations on the island of Crete, Greece (Kopanakis et al., 2012; Gerasopoulos et al., 2006) and in the range observed for urban background sites across Southern Europe (Karanasiou et al., 2014).

Despite the distance of the sampling site from pollution sources, concentrations exceeding the daily European Union's limit value (50 μg/m^3) were registered in 24 days (out of 278 sampling days) in 2007, and in 32 (out of 284 sampling days) in 2008, i.e. for 10% of the sampling period, being the highest concentrations due to Saharan dust events, as shown in (Marconi et al., 2014). The EU legal term of not exceeding the daily limit value of 50 μg/m^3 for the percentile 90.4 of the annual values was not respected in 2008 (when percentile 90.4 was 52.5 μg/m^3) and nearly reached in 2007 (when percentile 90.4 was 48.9 μg/m^3).

3.2 PM_{10} speciation

Average concentrations (and standard deviation) of the main measured elements/species for all the sampling period and in the different seasons are reported table 1. The determination of several elements by different techniques allowed performing a quality assurance analysis of data and studying the solubility of specific elements (Becagli et al., 2012), by comparing results on the total content as obtained by PIXE and on the soluble content as obtained by IC or ICP-AES.

Sea-salt and mineral dust contributions were estimated assuming the average composition of seawater and Earth's soil (Mason, 1966). In particular, sea-salt concentration (i.e. [sea-salt]) was evaluated, for every day, according to the expression:

$[\text{sea-salt}] = [\text{Cl}^-] + [\text{ssNa}^+] + [\text{ssCa}] + [\text{ssMg}] + [\text{ssK}] + [\text{ssSO}_4^{2-}]$

where $[\text{Cl}^-]$ is the Cl concentration measured by IC and Na, Mg, K, Ca, and SO_4^{2-} contributions due to sea-salt ($[\text{ssNa}^+]$, [ssMg,] [ssK], [ssCa] and $[\text{ssSO}_4^{2-}]$) are estimated according to the following equations:

$[\text{ssNa}^+] = [\text{Na}^+] - [\text{nssNa}^+] = [\text{Na}^+] - [\text{nssCa}] \cdot (\text{Na/Ca})_{\text{crust}} = [\text{Na}^+] - ([\text{Ca}] - [\text{ssCa}]) \cdot (\text{Na/Ca})_{\text{crust}}$

$[\text{ssCa}] = [\text{ssNa}^+] \cdot (\text{Ca/Na})_{\text{seawater}}$

$[\text{ssMg}] = [\text{ssNa}^+] \cdot (\text{Mg/Na})_{\text{seawater}}$

$[\text{ssK}] = [\text{ssNa}^+] \cdot (\text{K/Na})_{\text{seawater}}$

$[\text{ssSO}_4^{2-}] = [\text{ssNa}^+] \cdot (\text{SO}_4^{2-}/\text{Na})_{\text{seawater}}$

where $[\text{Na}^+]$ and [Ca] are the concentrations obtained respectively by IC and PIXE; $(\text{Na/Ca})_{\text{crust}}$ represents the mean Na/Ca ratio in the Earth crust, assumed to be 0.56 according to literature (Henderson and Henderson, 2009); $(\text{Ca/Na})_{\text{seawater}}$, $(\text{Mg/Na})_{\text{seawater}}$, $(\text{K/Na})_{\text{seawater}}$ and $(\text{SO}_4/\text{Na})_{\text{seawater}}$ are the mean elemental ratios in bulk seawater and are set to 0.038, 0.119, 0.037, and 0.253, respectively (Henderson and Henderson, 2009).

The contribution of mineral dust ([mineral dust]) was calculated as sum of the metal oxides for every day based on stoichiometric ratios (e.g., Nava et al., 2012):

$[\text{mineral dust}] = 1.35\,[\text{nssNa}^+] + 1.66\,[\text{nssMg}] + 1.89\,[\text{Al}] + 2.14\,[\text{Si}] + 1.21\,[\text{nssK}] + 1.40\,[\text{nssCa}] + 1.67\,[\text{Ti}] + 1.43\,[\text{Fe}]$

where “nss” stands for “non-sea-salt” (see previous equations) and [Al], [Si], [Ti], [Fe] are the elemental concentrations of Al, Si, Ti, Fe as measured by PIXE; the numerical coefficients account for the weight of the Oxygen atom in the main oxides of such elements in the average Earth crust.

According to this estimate, sea-salt and mineral dust contribute to PM_{10} in Lampedusa with 8.3 $\mu\text{g/m}^3$ and 5.8 $\mu\text{g/m}^3$ (corresponding to 26% and 18% of the PM_{10} mass) as average on the

2-year period, respectively. None of the components has a clear seasonality, and the temporal pattern of mineral dust shows several episodic peaks. Sea salt levels are of the same order as observed in other coastal Mediterranean sites. As concerns mineral dust, the observed concentrations are in the range observed for the crustal component in Mediterranean background sites (Querol et al., 2009), as well as consistent with the mean African dust contributions observed in Mediterranean urban and suburban sites (Pey et al., 2013), due to the character prevalently of long-range transport of this component.

Despite the remoteness of the site, not-negligible secondary aerosol levels characterize the PM_{10} in Lampedusa. Nitrate in Lampedusa accounted for 2.1 $\mu g/m^3$ as average on the 2-year period: this value appears to be slightly higher than in other Mediterranean Basin background sites (1.7 – 1.9 $\mu g/m^3$) and in rural and urban background sites in Italy, and on the lower edge of those measured in Central Europe and UK (2 – 4 $\mu g/m^3$) (Querol et al., 2009). Sulphate levels (3.6 $\mu g/m^3$ as average on the 2-year period, out of which 2.9 $\mu g/m^3$ are nss-sulphate) are also in the range reported for Central and Southern Europe and UK rural background stations (2 – 4 $\mu g/m^3$), although lower than in background sites in the Eastern Mediterranean Basin (5 – 6 $\mu g/m^3$), influenced by long range transport episodes from Eastern Europe (Querol et al., 2009).

MSA, a typical marker of biogenic activity, shows the typical seasonality with maxima during summer and minima in winter due to the seasonality in the emission of its precursor dimethylsulfide (DMS; Becagli et al., 2013).

As concerns the carbonaceous fraction of aerosol, data are available only for a very limited time (24 samples averaging on 24 to 72 h in the period 16 May-15 August 2007): in such period, on average, TC and EC accounted for 1.9 and 0.4 $\mu g/m^3$, i.e. for 8.0% and 1.5% of PM_{10} mass, respectively. Preliminary results on the 2011 campaign on 1-year-long data set estimate TC and EC levels as 9.6% and 0.1% of PM_{10} mass, thus confirming the order of magnitude of carbonaceous aerosol levels in Lampedusa as measured during the short 2007 campaign. In particular, EC appears to be a negligible component of PM10 in Lampedusa, and carbonaceous aerosol appears to be mainly organic; taking into account for non-C atoms in particulate organic matter (POM) by multiplying OC for a factor 2.1 as suggested by (Turpin and Lim, 2001) for nonurban sites, POM mass appears to contribute for about 20% of PM_{10} mass in Lampedusa.

The reconstructed mass, i.e. the sum of all the components determined by chemical analysis, corresponds to 61% of the gravimetrical mass. When adding to this value the estimated 20% of POM, the unaccounted mass usually attributed to water molecules is about 19%, in agreement with the 10 to 20% range reported in literature for coastal rural and Mediterranean background sites (Koçak et a., 2007; Pey et al., 2009; Querol et al., 2009). Nevertheless, some of the unaccounted mass may be partially attributed to carbonates, which were not assessed in this study.

3.3 PM_{10} sources identification by PMF

The PMF model was applied to the data set of mass concentration and chemical composition relative to the 562 samples collected in the years 2007-2008, considering 21 chemical species as measured by either PIXE (Mg, Al, Si, K, Ca, Ti, Mn, Fe, Cu, Br, Sr), ICP-AES (V_{sol}, Ni_{sol}) or IC (Na^+, NH_4^-, Cl^-, NO_3^-, SO_4^{2-}, Oxalates, Glycolate, MSA); all such variables are “good”, according to the signal-to-noise (S/N) ratio criterion by (Paatero and Hopke, 2003). The soluble fraction of V and Ni (V_{sol}, Ni_{sol}) was used instead of their total fraction due to the lower DLs of ICP-AES compared to PIXE, and because it is a more representative marker for anthropogenic sources (Becagli et al., 2012). Missing data were less than 1% of the total number of samples for all chemical species, except soluble elements (5%) and Cu (9%).

A seven-factor solution, with FPEAK value 0.1, was selected, on the basis of the Q value, observed residual distributions, factor edges, physical sense of the source profiles and temporal evolutions (F and G matrixes (Paatero, 1997)); observed relative ratios and enrichment factors for the different sources are consistent with literature data, strengthening the results of the analysis. Briefly, the analysis allowed the identification of 7 different sources which are identified as sea-salt, mineral dust, biogenic emission aerosol, secondary nitrate particles, secondary sulphate particles, primary particulate ship emissions, and combustion emission aerosol (see the following sections). All together, these sources reconstruct the measured gravimetric mass within 4%. The six-factor solution was excluded, as it did not separate the secondary nitrate source from the combustion emission one. The eight-factor solution was also discarded, as it was identifying an unlikely source related primarily to Ca and Sr (44% and 21% explained variations, respectively): the hypothesis of facing a local dust resuspension source was discarded as the profile of this source did not contain any contributions from other crustal elements (such as Ca, Si and Al); further, the temporal profile of this factor is very similar to the mineral dust one (in particular, it shows the same peaks during Saharan dust advection episodes).

The seven sources are described in the following sections. Profiles are reported in Figure 3: the left y-axis displays the fraction of the elemental mass concentration, reported in the graph as blue column, whereas the right y-axis refers to the explained variation of each element, depicted as red squares (the contribution of one element in all the profiles sum up to one, when the variation of the element is completely reconstructed by the model). Error bars on the fraction of the elemental mass concentration represent the computed errors as provided by the PMF2 model. These estimates take into account the uncertainties on the input data and the application of non-negativity criteria; nevertheless, they do not consider rotational ambiguity (Paatero et al., 2014), which was in any case investigated by systematically exploring solutions with different FPEAK values (see Supplementary Material), according to a literature approach (Vecchi et al., 2008). The evolution of the daily contribution of each identified source is shown in Figure 4.

3.3.1 Sea-salt

Na^+, Cl^-, Mg, K and Br are the characterizing elements for this factor (figure 3, panel a); most of their mass concentration is explained by this source (explained variations: 64%, 83%, 48%, 30% and 61% respectively). Some SO_4^{2-} is also present. The elemental ratios are in good agreement with those measured in marine water, suggesting a common marine origin for the species characterizing this factor. More in detail, the source profile elemental ratios are reported in Table 2 together with the sea salt literature elemental ratio (Henderson and Henderson, 2009). Thus, this factor of the PMF is identified with the primary marine aerosol, sea salt aerosol.

The temporal evolution shows no clear seasonality, as it can be expected for this source, since the sampling site is located directly on the coast and sea-salt aerosol is known to be strongly related to wind intensity (Kishcha et al., 2011).

3.3.2 Mineral dust

Several crustal elements such as Al, Si, Ti, Mn, Fe, Sr, Ca, K an Mg characterize this factor (figure 3, panel b). This source reconstructs almost completely the mass concentration of some of these elements, such as Al, Si and Ti (more than 80% of their signal).

Enrichment factors (EF) with respect to Al in this profile were calculated using the average Earth's soil composition reported by (Mason, 1966) and are reported in Table 3.

The values of these EFs, all close to 1 (with a moderate enrichment only for Ca and Sr which is usually associated with Ca in carbonates), strengthen the identification of this source as "mineral dust".

The temporal evolution of this factor shows no clear seasonality, being dominated by many narrow peaks. Sixty-hour backward trajectories ending at Lampedusa at 50 m a.s.l. corresponding to the start, middle, and end time of the sampling interval were calculated for the peaks in PM_{10} concentrations due to mineral dust larger than the 95° percentile (about 32 $\mu g/m^3$), using the NOAA Air Resource Laboratory HYSPLIT transport model (Draxler and Rolph, 2012). The analysis showed that in about 86% of the cases at least one of the three trajectories associated to the sampling overpassed Northern Africa (see Figure 5). This result should be read taking into account the uncertainties in the HYSPLIT trajectories due to the lack of meteorological measurements in the examined region, the low model horizontal resolution, and the possible rapid temporal variation of the air masses during the sampling interval. No relevant difference in the available crustal markers ratios was observed in correspondence of African dust transport episodes, suggesting a similar chemical composition for the Lampedusa soil and the African dust (limitedly to the measured elements), or a negligible impact of local dust. In fact, enrichments in Ca with respect to the average Earth's soil composition are reported for dust originating from different African areas, e.g. Western Sahara and Moroccan Atlas, due to the high content of minerals such as calcite and dolomite (Avila et al., 1997; Coz et al., 2009). An enhancement of Ca amounts for dust originating from the Algeria-Tunisia sector was shown by (Marconi et al., 2014).

The seasonality of African desert dust advection episodes in Lampedusa was discussed in a recent study (Marconi et al., 2014) based on a larger data-set (June 2004 – December 2010), in which ground level aerosol concentrations are compared with aerosol optical depth measurements routinely performed at the Station for Climate Observations of Lampedusa, providing information on the dust content in the entire air column above the sampling site. African desert dust transports often occur above the boundary layer (mainly in summer); in fact, despite the strong seasonality observed for the aerosol optical depth, at the ground level no evident seasonal trend was observed for PM_{10} or crustal markers, in agreement with the mineral dust temporal pattern obtained by PMF on the 2007-2008 data-set. In particular, as shown by (Marconi et al., 2014), while the aerosol optical depth and the frequency of occurrence of vertically integrated dust events peak in summer, a relative minimum of PM_{10} concentration and its frequency of occurrence is found in the months of June-July.

3.3.3 Biogenic emissions

This factor is mainly characterized by MSA (Methanesulfonic Acid), and explains almost completely (87%) its mass concentration. A small percentage (6%) of the total mass of SO_4^{2-} is also accounted by this source, and constitutes however the prevalent absolute mass contribution to this factor.

MSA is used as a tracer for biogenic sulphur emissions (from phytoplankton processes), as it is solely produced by oxidation of dimethylsulfide (DMS). The evaluation of the nssSO_4^- emitted by the biogenic source, $(nss\text{-}SO_4^{2-})_{bio}$, suffers by the variability of the $(nss\text{-}SO_4^{2-})_{bio}$ /MSA emission ratio as this depends on the latitude, the NO_x levels and the temperature (Seinfeld and Pandis, 1998; Bates et al., 1992); this is especially true for the Mediterranean basin, where only a maximum value for such ratio has been estimated in previous studies (in Crete) (Mihalopoulos et al., 1997; Kouvarakis and Mihalopoulos, 2002). The observed SO_4^{2-} /MSA ratio in this source, 11.3, is only slightly higher than the aforementioned estimated maximum value (10) and it could be considered as representative for the $(nss\text{-}SO_4^{2-})_{bio}$/MSA ratio for the biogenic emissions in the Central Mediterranean basin. By using the value of 11.3 we found that in summer (JJA), when biogenic sulphur emission is at its maximum, 0.5 μg m^{-3}

of SO_4^{2-}, corresponding to 11% of total SO_4^{2-}, arise from a natural source. This result confirms the order of magnitude of the biogenic sulphur contribution during summer estimated as 17% by (Kouvarakis and Mihalopoulos, 2002) by observations and modelling.

The strong seasonality observed for this factor, with minima during winter and maxima in summer, is also supporting its attribution to the biogenic emissions source. A recent study investigated the role of biogenic aerosols in the PM at Lampedusa (Becagli et al., 2013) with respect to the phytoplancton productivity, suggesting that the seasonal evolution of methanesulfonate, with a very evident summer maximum, is mainly driven by phytoplankton physiology and cell stress factors, such as high irradiance and shallow depth of the marine upper mixed layer.

3.3.4 Secondary nitrate

This factor is characterized by NO_3^- and Na^+, with the mass concentration of NO_3^- being explained almost for the 80% by it.

The ionic balance for this source is neutral, when taking into account NO_3^- and the two cations Na^+ and Mg^{2+}, as in a marine environment the neutralization of HNO_3 can occur to a large extent on sea-salt components (Bardouki et al., 2003; Metzger et al., 2006).

The temporal evolution shows a small seasonality, with somewhat larger values during summer. A similar seasonal behaviour was observed by (Querol et al., 2009) in Eastern Mediterranean Basin (EMB) sites. The same study evidenced that in the EMB nitrate is mainly present in the coarse mode, chemically bound to alkaline ion species, while in the Western Mediterranean Basin (WMB) it is largely in the fine mode, as it is most frequently present as ammonium nitrate. In Lampedusa, as in the EMB, the observed seasonality appears to be mainly regulated by the combination of nitrates with sea-salt cations (Metzger et al., 2006), while in the WMB nitrate is dominated by a strong opposite seasonality, with maxima during winter, due to both the instability of ammonium nitrate in warm environments and intense nitrate episodes in late winter.

3.3.5 Secondary sulphate

NH_4^+, SO_4^{2-}, and Oxalates are the characterizing elements for this source, with most of their signals explained by this factor (explained variations are 87%, 54%, and 45%, respectively). The major absolute contribution to the profile is given by SO_4^{2-}; the SO_4^{2-}/NH_4^+ ratio of 3.4 indicates that both the compounds $(NH_4)HSO_4$ and $(NH_4)_2SO_4$ are present.

The temporal evolution shows maxima during summer, when the marine boundary layer is more stable and the photochemistry leading to the production of secondary aerosols is enhanced. The same behaviour was observed by (Querol et al., 2009) for sulphate both at Eastern and Western Mediterranean sites. Further, it is worthy to note that sulphate neutralization with NH_4^+ may leave very low amounts of NH_3 available for the neutralization of nitrate, which thus occurs favourably on sea-salt aerosol (see 3.2.4).

3.3.6 Primary particulate ship emissions

This factor explains most of the mass of V_{sol} and Ni_{sol}, even if the predominant mass contributions are from Na^+ and SO_4^{2-}. V and Ni have been clearly recognized as markers of heavy oil combustion, and characteristic V/Ni ratios ranging from 2.5 to 3.5 have been reported for ships emissions (Mazzei et al., 2008; Viana et al., 2009; Pandolfi et al., 2011). Further, both V and Ni were found to have roughly the same solubility (80% and 77%, respectively) when originated by heavy oil combustion, in the mild extraction condition (HNO_3 – pH 1.5) used for ICP-AES extraction (Becagli et al., 2012). The V_{sol}/Ni_{sol} ratio for this source is 3.40, in good agreement with the aforementioned literature data. Moreover, the interpretation of this factor as "primary ship emissions" is strengthened by the fact that the observed SO_4^{2-}/V_{sol} ratio (6.2 w/w;

as V has been found to have a 80% solubility in ships exhausts, such value corresponds to a SO_4^{2-}/V ratio of 5.0) is of the same order of magnitude as the ones reported by (Agrawal et al., 2008) for the particulate matter freshly emitted from the main engine of an ocean going container vessel (SO_4^{2-}/V ranging from 8.9 to 11.9 depending on the engine operating conditions for the considered vessel). Much higher SO_4^{2-}/V values are reported when secondary aerosols (mainly SO_4^{2-}) are formed from the oxidation of the gaseous precursors (e.g., SO_2) (Becagli et al., 2012).

A clear seasonal evolution, with maxima during summer, is evident for this source; this is in agreement with the temporal evolution of ship emissions markers (Ni_{sol}, V_{sol}, $nssSO_4^{2-}$) observed by (Becagli et al., 2012) on a larger data set of samples collected at the same Lampedusa site (years 2004-2008). The authors explained the temporal evolution of these markers as due to three possible causes: a) an increased photochemical activity in summer leading to a faster production of secondary aerosols; b) a stronger stability of the marine boundary layer during summer, leading to an increase of their concentrations at the ground level; c) prevalent winds from the Strait of Sicily (one of the main ship paths) during summer. Due to the primary origin of this factor, such seasonal behaviour appears to be more probably linked to the two latter phenomena.

3.3.7 Combustion emissions

Several compounds, as K, Cu, NO_3^-, SO_4^{2-} and short carboxilic acids as Oxalates and Glycolates, whose signal is mostly explained by this source, characterize this factor. K and SO_4^{2-} are commonly associated with biomass burning, and short carboxilic acids have been recently associated with coal/waste/biomass burning (Wang et al., 2007). Enhancements of Cu in the aerosol produced by wood combustion have also been reported by several studies

(Dall'Osto et al., 2013; Nava et al., 2015). Therefore this factor has been interpreted as a generic combustion source, which includes biomass burning.

The temporal evolution (Figure 4) of this factor shows no clear seasonality, even if important contributions during summer may be observed and may be linked to the more frequent occurrence of fires in the Mediterranean region. During spring and autumn the contributions from this source are generally low, while several high contribution days may be observed during winter. Figure 6 shows the combined evolution of the desert dust and combustion emissions contributions to PM_{10}, and some selected cases with airmass trajectories and satellite observations of active fires. Most of the winter cases characterized by elevated contributions of combustion sources display also a high contribution from the mineral dust source (see Figure 6). The analysis of the backtrajectories shows that these days were mostly interested by African dust advection episodes. Several studies report that dust particles plumes from the Saharan area also export biomass-burning particles, mainly during the dry winter season, as well as emissions from refineries (Tesche et al., 2011; Rodriguez et al., 2011). Further, small fires, often occurring in biomes as croplands, wooded savannas and tropical forests, are usually below the detection limit of the current generation of surface reflectance/thermal imagery instruments (Randerson et al., 2012). Therefore, winter contributions from this source are likely to be mainly due to small scale biomass burning activity in north Africa; nonetheless, some winter peaks of this source appear also connected with fires and/or biomass burning activity in Central-Eastern Europe (e.g., 13-15/3/2007, Figure 6).

Summer peaks have been clearly connected by backtrajectory analysis to fires mainly in South Italy and Sicily, thus supporting the interpretation of this factor as a combustion source, with a main contribution from biomass burning.

3.3.8 Combustion emission source identification: additional data

EC and OC are produced in combustion processes of both fossil fuels and biomasses, while OC may have also a biogenic origin. Therefore, EC and, to a smaller extent, OC are good markers of combustion sources, while additional information from other chemical tracers (such as K, levoglucosan, glycolates or radiocarbon (Bernardoni et al., 2013)) may help for the assessment of the burnt fuel (biomass or fossil). Despite OC is a major aerosol component and EC is an important combustion tracer, a recent study has demonstrated that the lack of data for these species does not significantly alter PMF results provided that a complete elemental and ionic speciation is available, so that other markers tracing combustion emissions are available (Lucarelli et al., 2015). Nevertheless, a comparison of the results for the combustion source as derived by the PMF analysis with the available EC/OC data was performed. As previously reported, additional data on the carbonaceous fractions in PM_{10} are available for limited periods in the years 2007-2008. In particular, 24 samplings of PM_{10} on quartz filters for EC/OC analysis were performed from 16 May to 15 August 2007 with integration times ranging from 24 to 72 h. The starting time of the sampling was set in the morning/early-afternoon (between 8 am and 2 pm) due to manual filter change operations. In Figure 7, the EC and OC contents are plotted together with the estimates of the contributions from the combustion emission source as obtained by PMF. As may be seen, EC and OC are highly correlated with the combustion emission contribution estimated by the PMF, thus strengthening the attribution of the seventh PMF factor to a combustion source. Small discrepancies, as the one occurring at the beginning of July, may be attributed to episodic important contributions to EC and OC from heavy oil combustion, that is from the primary particulate ship emission source, also reported in Figure 7.

The availability of a complete EC-OC data set for the future campaigns will add valuable information on the sources and contributions of the carbonaceous aerosol component.

3.4 PM_{10} source apportionment

Figures 8 and 9 report the relative and absolute seasonal contributions of the seven identified sources (winter – December, January, February; spring – March, April, May; summer – June, July, August; fall – September, October, November). During all the seasons, natural sources (seas-salt, mineral dust, and biogenic emissions) give the largest contribution to PM_{10}, accounting for a minimum of 62% in spring to a maximum of 76% during fall. The maximum relative and absolute contribution of sea-salt is observed in winter, while relative contributions during the other seasons are comparable. This is consistent with a higher wind velocity during the winter months (7.4 m/s, versus 5.6 m/s in summer, 6.5 m/s in spring, and 6.1 m/s in fall during 2007 and 2008).

The mineral dust maximum relative contribution is found during fall (37%), and is around 20% in the other seasons. As expected, the maximum relative contribution of biogenic emissions is during summer, and is negligible in winter.

Among the anthropogenic sources, primary particulate ship emissions and secondary sulphate display a clear and similar seasonality, with maxima in summer. No significant dependence on the season is observed for the relative contributions of secondary nitrate and combustion emissions. It is worth to note that the not explained mass is around 10% across the seasons.

The annual average relative contributions are reported with their uncertainties in Figure 10: the main contribution to aerosol comes from sea-salt, accounting for 40% of the mass; the second contribution is from mineral dust (25%). Taking into account also the biogenic emissions, accounting for 4% of the mass, the contribution of natural sources to the PM_{10} in Lampedusa is estimated to be around 68% on average. As concerns secondary nitrates and sulphates, they are estimated to contribute by 9% and 11% to the total PM_{10}, respectively.

Finally, primary particulate ship emissions have been observed to give an average 4% contribution, while 5% of PM_{10} was found to be due to combustion emissions. Uncertainties on the contributions were estimated propagating the uncertainties obtained by the PMF model on the G matrix.

In absolute terms, the following contributions were estimated: sea-salt, 12.9 ± 1.1 $\mu g/m^3$; mineral dust, 7.8 ± 0.5 $\mu g/m^3$; biogenic emissions, 1.1 ± 0.2 $\mu g/m^3$; secondary nitrate, 2.8 ± 0.3 $\mu g/m^3$; secondary sulphate, 3.4 ± 0.4 $\mu g/m^3$; primary particulate ship emissions, 1.2 ± 0.2 $\mu g/m^3$; combustion emissions, 1.5 ± 0.3 $\mu g/m^3$.

3.4.1 Evaluation of the total contribution from ship emissions to PM_{10} in Lampedusa

An estimate of the contribution of the shipping emissions to the secondary sulphate formation was performed following previous studies (Kim and Hopke, 2008; Viana et al., 2009), based on the observed correlation between the daily contributions from the primary particulate ship emission source and those from the secondary sulphate source as assessed by PMF analysis. The contributions from these two sources are plotted one against the other in Figure 11: the solid line represents the minimum amount of secondary sulphate that is expected to be associated to the observed primary particulate from ship emissions. Such line was graphically drawn aiming at excluding outliers and its slope indicates that, at the receptor site, at least 0.9 $\mu g/m^3$ of secondary sulphate are expected per unit of detected primary particulate from ship emissions. Therefore, primary particles contribute by 50% or less to the total PM_{10} originating from ship emissions. (Kim et al., 2008) reported about 0.8 $\mu g/m^3$ of secondary sulphate per 1 $\mu g/m^3$ of primary oil combustion particles in $PM_{2.5}$ in 3 sites in Seattle (WA, USA). A larger ratio (about 2.1) was found by (Viana et al., 2009) for PM_{10} in Melilla (Spain). Both oil combustion particles and secondary aerosols are found mainly in the fine aerosol fraction, therefore the ratio between the two components (secondary sulphate and primary particulate) of the ship emissions source is likely to be roughly the same for $PM_{2.5}$ and PM_{10}. It must be pointed out however that we retrieved a minimum value, and the actual contribution of secondary sulphate depends on many factors and, in many cases, may be much higher than the limit.

Taking into account this minimum secondary sulphate contribution, we derive a minimum SO_4^{2-}/V_{sol} ratio of about 190 for ship emissions (primary particulate + secondary sulphate). It is worthy to note that a SO_4^{2-}/V_{sol} ratio = 200 was proposed as characteristic lower ratio for ship emissions from a previous study performed at Lampedusa (Becagli et al., 2012) on a more extended dataset (June 2004 – December 2008).

Further, ship emissions on the whole (primary particulate + secondary sulphate) are estimated to contribute to PM_{10} in Lampedusa by approximately 7% (about 4% primary particles and 3% secondary sulphate). These values confirm the order of magnitude of the estimated impact of ship emissions in European coastal areas, which is reported to be around 1–7% (EEA techn. report, 2013).

3.4.2 Comparison of contribution estimates by PMF and speciation

The PMF estimates of the contributions from sea-salt and mineral dust were compared with those obtained according to the average composition of seawater and Earth's soil (paragraph 3.2).

The mineral dust estimate from the PMF analysis is about 30% higher than the crustal content calculated as the metal oxides sum. It must be pointed out that no information on carbonates is available, and that the used analytical techniques are not sensitive to the Oxygen content, thus the estimated mineral dust mass is based on the assumption of an oxygen fraction according to the prevalent oxides of the crustal elements. This assumption is obviously an approximation as the real mineral dust composition may differ from it; as an example, this approach may underestimate the mineral dust contribution in presence of a significant amount of carbonates. Nevertheless, PMF may slightly overestimate the source contribution as a consequence of some profile interferences (Mazzei et al., 2008): in this case, the PMF retrieval associated a small amount of SO_4^{2-} and Cl^- to the crustal dust profile, probably due to their co-linearity in case of long-range transport episodes.

Coming to sea-salt, the stoichiometric approach gives an estimate of the average contribution of 8.3 μg/m^3, to be compared with the PMF estimated contribution for the sea-salt source of 12.9 μg/m^3. Since all the sea-salt elements are measured, this discrepancy is likely to be due to other compounds not visible with the applied analytical techniques, such as water or, to a lesser extent, organic compounds. In fact, although gravimetric measurements are performed in a controlled atmosphere (50% relative humidity, 25°C), some water may endure and it is likely to be bound to hygroscopic aerosol components such as sea-salt; this is in agreement with recent studies that have shown water exists in ambient aerosol also at low relative humidity (Plinis et al., 2014; Engelhart et al., 2011). Therefore, taking into account for water, the PMF contribution from the sea-salt source may be possibly split in two contributions, namely “dry sea-salt” and “H_2O”, accounting for about 26% and 14% of the PM_{10} mass in Lampedusa, respectively. This estimate lays in the 10 to 20% range reported in literature for unaccounted mass in Mediterranean background/rural sites (Koçak et a., 2007; Pey et al., 2009; Querol et al., 2009), which is generally attributed to water molecules of moisture.

In any case, it has to be pointed out that some variability in the chemical profiles of the sea-salt factors across the Mediterranean is reported in literature, due to possible reactions occurring in the atmosphere: for Mediterranean coastal sites, some papers report, as for this work, a sea-spray composition in agreement with the marine water one (e.g., Koçak et al., 2007; Amato et al. 2015); other papers report a Cl^- depletion (i.e. Cl^-/Na^+ ratios lower than in marine water) at coastal sites (Koulouri et al., 2008) as well as in open Mediterranean sea (Schembari et al., 2014).

4. Conclusions

On average, each of the sources “primary particulate ship emissions”, “biogenic emissions” and “combustion emissions” contributes by about 5% to the total PM_{10} mass; “secondary nitrate” and “secondary sulphate” account for about 10% each; the “mineral dust” contribution is around 25%, while “sea-salt” constitutes about 40% of the PM_{10}. According to a stechiometric approach, the latter may possibly split in two contributions, namely “dry sea-salt” and “H_2O”, accounting for roughly 25% and 15% of the PM_{10} mass in Lampedusa, respectively. Further, about one third of the total contribution of secondary sulphate appears to originate from ship emissions. Large variations in absolute and relative contributions are found and appear to depend on the season and on transport episodes.

Improvements to this source apportionment will be possible taking into account for the carbonaceous fraction (no extensive dataset is available for it for the considered years, 2007 and 2008).

Acknowledgements

This work has been supported by the SNUMMASS and NextData projects, and the RITMARE Flagship Project funded by Italian Ministry of University and Research. The measurements presented here are preparatory to Chemistry-Aerosol Mediterranean Experiment project (ChArMEx), which is the atmospheric component of the French multidisciplinary program MISTRAL.

References

Amato, F., Alastuey, A., Karanasiou, A., Lucarelli, F., Nava, S., Calzolai, G., Severi, M., Becagli, S., Gianelle, V. L., Colombi, C., Alves, C., Custódio, D., Nunes, T., Cerqueira, M., Pio, C., Eleftheriadis, K., Diapouli, E., Reche, C., Minguillón, M. C., Manousakas, M., Maggos, T., Vratolis, S., Harrison, R. M. and Querol, X.: AIRUSE-LIFE+: a harmonized PM speciation and source apportionment in 5 Southern European cities, Atmos. Chem. Phys. Discuss., 15, 23989-24039, 2015.

Argyropoulos, G., Manoli, E., Kouras, A. and Samara, C.: Concentrations and source apportionment of PM_{10} and associated major and trace elements in the Rhodes Island, Greece, Sci. Tot. Env., 432, 12-22, 2012.

Artuso, F., Chamard, P., Piacentino, S., Sferlazzo, D. M., De Silvestri, L., di Sarra, A., Meloni, D. and Monteleone, F.: Influence of transport and trends in atmospheric CO_2 at Lampedusa, Atmos. Environ., 43, 3044–3051, 2009.

Ault, A. P., Gaston, C. J., Wang, Y., Dominguez, G., Thiemens, M. H., and Prather, K. A.: Characterization of the single particle mixing state of individual ship plume events measured at the port of los Angeles, Environ. Sci. Technol., 44, 1954–1961, 2010.

Avila, A., Queralt-Mitjans, I. and Alarcon, M.: Mineralogical composition of African dust delivered by red rains over northeastern Spain, J. Geophys. Res., 108, 21977–21996, 1997.

Bardouki, H., Liakakou, H., Economou, C., Sciare, J., Smolík, J., Ždímal, V., Eleftheriadis, K., Lazaridise, M., Dyef, C. and Mihalopoulos, N., Chemical composition of size-resolved atmospheric aerosols in the eastern Mediterranean during summer and winter, Atm. Env. 37, 195–208, 2003.

Bates, T.S., Calhoun, J.A. and Quinn, P.K.: Variations in the concentration ratio of methane-sulfonate to sulfate in marine aerosol particles over the South Pacific Ocean, J. Geophys. Res. 97, 9859-9865, 1992.

Becagli, S., Ghedini, C., Peeters, S., Rottiers, A., Traversi, R., Udisti, R., Chiari, M., Jalba, A., Despiau, S., Dayan, U., and Temara. A.: MBAS (Methylene Blue Active Substances) and LAS (Linear Alkylbenzene Sulphonates) in Mediterranean coastal aerosols: sources and transport processes, Atmos. Environ., 45, 6788–6801, 2011.

Becagli, S., Sferlazzo, D. M., Pace, G., di Sarra, A., Bommarito, C., Calzolai, G., Ghedini, C., Lucarelli, F., Meloni, D., Monteleone, F., Severi, M., Traversi, R., Udisti, R.: Evidence for heavy fuel oil combustion aerosols from chemical analyses at the island of Lampedusa: a possible large role of ships emissions in the Mediterranean, Atmos. Chem. Phys., 12, 3479–3492, 2012.

Becagli, S., Lazzara, L., Fani, F., Marchese, C., Traversi, R., Severi, M., di Sarra, A., Sferlazzo, D., Piacentino, S., Bommarito, C., Dayan, U. and Udisti, R.: Relationship between methanesulfonate (MS-) in atmospheric particulate and remotely sensed phytoplankton activity in oligo-mesotrophic Central Mediterranean Sea, Atmos. Environ., 79, 681-688, 2013.

Bernardoni, V., Calzolai, G., Chiari, M., Fedi, M., Lucarelli, F., Nava, S., Piazzalunga, A., Riccobono, F., Taccetti, F., Valli, G. and Vecchi, R.: Radiocarbon analysis on organic and elemental carbon in aerosol samples and source apportionment at an urban site in Northern Italy, J. Aer. Sci. 56, 88-99, 2013

Calzolai G., Chiari, M., García Orellana, I., Lucarelli, F., Migliori, A., Nava, S., and Taccetti, F.: The new external beam facility for environmental studies at the Tandetron accelerator of LABEC, Nucl. Instr. & Meth. B, 249, 928–931, 2006.

Calzolai, G., Bernardoni, V., Chiari, M., Fedi, M., Lucarelli, F., Nava, S., Riccobono, F., Taccetti, F. Valli, G. and Vecchi, R.: The new sample preparation line for radiocarbon measurements on atmospheric aerosol at LABEC, Nucl. Instr. & Meth. B 269, 203-208, 2011.

Campbell, J.L., Boyd, N.I., Grassi, N., Bonnick, P. and Maxwell, J.A.: The Guelph PIXE software package IV. Nucl. Instr. & Meth. B 268, 3356-3363, 2010.

Castelli, L., Giuntini, L., Taccetti, F., Barzagli, E., Civita, F., Czelusniak, C., Fedi, M.E., Gelli, N., Grazzi, F., Mazzinghi, A., Palla, L., Romano, F.P. and Mando', P.A.: New criterion for in situ, quick discrimination between traditionally maintained and artificially restored Japanese swords (katanas) by XRF spectroscopy, X-Ray Spectrometry 42, 537-540, 2013.

Coz, E., Gomez-Moreno, F.J., Pujadas, M., Casuccio, G.S., Lersh, T.L. and Artinao, B.: Individual particle characteristics of North African dust under different long-transport scenarios, Atmos Environ, 43, 1850–1863, 2009.

Cusack, M., Pérez, N., Pey, J., Alastuey, A. and Querol, X.: Source apportionment of fine PM and sub-micron particle number concentrations at a regional background site in the western Mediterranean: a 2.5 year study, Atmos. Chem. Phys., 13, 5173–5187, 2013.

Dayan, U., Heffter, J. L., and Miller J. M.: Meteorological and climatological data from surface and upper measurements for the assessment of atmospheric transport and deposition of pollutants in the Mediterranean Basin: Part B: Seasonal distribution of the planetary boundary layer depths over the Mediterranean Basin, UNEP. Mediterranean Action Plan Technical Reports Series no. 30, Athens, Greece, 1989.

Dall'Osto, M., Querol, X., Amato, F., Karanasiou, A., Lucarelli, F., Nava, S., Calzolai, G., and Chiari, M.: Hourly elemental concentrations in PM2.5 aerosols sampled simultaneously at urban background and road site during SAPUSS – diurnal variations and PMF receptor modelling, Atmos. Chem. Phys., 13, 4375– 4392, 2013.

Di Biagio, C., di Sarra, A., Meloni, D., Monteleone, F., Piacentino, S. and Sferlazzo, D.: Measurements of Mediterranean aerosol radiative forcing and influence of the single scattering albedo, J. Geophys. Res., 114, D06211, doi: 10.1029/2008JD011037, 2009.

Di Iorio, T., di Sarra, A., Sferlazzo, D. M., Cacciani, M., Meloni, D., Monteleone, F., Fuà, D. and Fiocco, G.: Seasonal evolution of the tropospheric aerosol vertical profile in the central Mediterranean and role of desert dust, J. Geophys. Res., 114, D02201, doi: 10.1029/2008JD010593, 2009.

di Sarra, A., Di Biagio, C., Meloni, D., Monteleone, F., Pace, G., Pugnaghi, S. and Sferlazzo, D.: Shortwave and longwave radiative effects of the intense Saharan dust event of 25-26 March, 2010, at Lampedusa (Mediterranean sea), J. Geophys. Res., 116, D23209, doi: 10.1029/2011JD016238, 2011.

Draxler, R. R. and Rolph, G. D.: HYSPLIT (HYbrid Single-Particle Lagrangian Integrated Trajectory), online, Silver Spring. MD. Model access via NOAA ARL READY Website: http://www.arl.noaa.gov/ready/hysplit4.html, 2003.

Engelhart, G.J., Hildebrandt, L., Kostenidou, E., Mihalopoulos, N., Donahue, N.M., Pandis, S.N., Water content of aged aerosol, Atmos. Chem. Phys. 11, 911-920 (2011)

European Environment Agency, The impact of international shipping on European air quality and climate forcing, EEA Technical report, No 4/2013, ISSN 1725-2237, 2013

Escudero, M., Querol, X., Avila, A. and Cuevas, E.: Origin of the exceedances of the European daily PM limit value in the regional background areas of Spain, Atmos. Environ., 41, 730-744, 2007.

Fedi, M.E., Caforio, L., Mandò, P.A., Petrucci, F. and Taccetti, F.: May ^{14}C be used to date contemporary art?, Nucl. Instr. and Meth. B 294, 662-665, 2013.

Gerasopoulos, E., Kouvarakis, G., Babasakalis, P., Vrekoussis, M., Putaud, J.-P. and Mihalopoulos, N.: Origin and variability of particulate matter (PM_{10}) mass concentrations over the Eastern Mediterranean, Atm. Env. 40, 4679-4690, 2006.

Gómez-Amo, J. L., Estellés, V., di Sarra, A., Pedrós, R., Utrillas, M.P., Martínez- Lozano, J. A., González-Frias, C., Kyrö, E. and Vilaplana, J.M.: Operational considerations to improve total ozone measurements with a Microtops II ozone monitor, Atmos. Meas. Techn., 5, 759–769, 2012.

Henderson, P. and Henderson, G. M.: Earth science data, Cambridge University Press, 92–97, 2009.

Henne, S., Brunner, D., Folini, D., Solberg, S., Klausen, J. and Buchmann, B.: Assessment of parameters describing representativeness of air quality in-situ measurement sites, Atmos. Chem. Phys., 10, 3561-3581, 2010.

Hildebrandt, L., Kostenidou, E., Lanz, V. A., Prevot, A. S. H., Baltensperger, U., Mihalopoulos, N., Laaksonen, A., Donahue, N. M. and Pandis, S. N.: Sources and atmospheric processing of organic aerosol in the Mediterranean: insights from aerosol mass spectrometer factor analysis, Atmos. Chem. Phys., 11, 12499-12515, 2011.

Im, U., Markakis, K., Koçak, M., Gerasopoulos, E., Daskalakis, N., Mihalopoulos, N., Poupkou, A., Kındap, T., Unal, A. and Kanakidou, M.: Summertime aerosol chemical composition in the Eastern Mediterranean and its sensitivity to temperature, Atm. Env. 50 164-173, 2012.

IPCC: Climate Change 2007: The Physical Science Basis, Contri- bution of Working Group I to the Fourth Assessment Report of the IPCC, ISBN 978 0521 88009-1 Hardback; 978 0521 70596-7 Paperback, 2007.

Kim, E. and Hopke, P. K.: Source characterization of ambient fine particles at multiple sites in the Seattle area, Atmospheric Environment, 42, 6047-6056, 2008.

Kishcha P., Nickovic, S., Starobinets, B., di Sarra, A., Udisti, R., Becagli, S., Sferlazzo, D., Bommarito, C. and Alpert, P.: Sea-salt aerosol forecasts compared with daily measurements at the island of Lampedusa (Central Mediterranean), Atmos. Res., 100, 28–35, 2011.

Koçak, M., Mihalopoulos, N. and Kubilay, N.: Chemical composition of the fine and coarse fraction of aerosols in the northeastern Mediterranean, Atmos. Env., 41, 7351-7368, 2007

Kopanakis, I., Eleftheriadis, K., Mihalopoulos, N., Lydakis-Simantiris, N., Katsivela, E., Pentari, D., Zarmpas, P. and Lazaridis, M.: Physico-chemical characteristics of particulate matter in the Eastern Mediterranean, Atmospheric Research 106, 93–107, 2012.

Koulouri, E., Saarikoski, S., Theodosi, C., Markaki, Z., Gerasopoulos, E., Kouvarakis, G., Makela, T., Hillamo, R. and Mihalopoulos, N.: Chemical composition and sources of fine and coarse aerosol particles in the Eastern Mediterranean. Atmos. Environ. 42, 6542–6550, 2008.

Kouvarakis G. and Mihalopoulos, N.: Seasonal variation of dimethylsulfide in the gas phase and of methanesulfonate and non-sea-salt sulfate in the aerosol phase measured in the Eastern Mediterranean atmosphere, Atmos. Environ. 36, 929-938, 2002.

Li, Z. and Aneja, V. P.: Regional analysis of cloud chemistry at high elevations in the eastern United States, Atmos. Environ., 26A, 2001–2017, 1992.

Lucarelli, F., Nava, S., Calzolai, G., Chiari, M., Udisti, R., and Marino, F.: Is PIXE still a useful technique for the analysis of atmospheric aerosols? The LABEC experience, X-Ray Spectrometry, 40, 162–167, 2011.

Lucarelli, F., Nava, S., Calzolai, G., Chiari, M., Giannoni, M., Traversi, R. and Udisti R.: On the autarchic use of solely PIXE data in particulate matter source apportionment studies by receptor modeling, Nucl. Instr. & Meth. B, http://dx.doi.org/10.1016/j.nimb.2015.08.019, 2015.

Marconi, M., Sferlazzo, D.M., Becagli, S., Bommarito, C., Calzolai, G., Chiari, M., di Sarra, A., Ghedini, C., Gómez-Amo, J.L., Lucarelli, F., Meloni, D., Monteleone, F., Nava, S., Pace, G., Piacentino, S., Rugi, F., Severi, M., Traversi, R. and R. Udisti: Saharan dust aerosol over the Central Mediterranean Sea: optical columnar measurements vs aerosol load, chemical composition and markers solubility at ground level, Atmos. Chem. Phys., 14, 2039–2054, 2014.

Mason, B.: Principles of Geochemistry, third ed., Wiley, New York, 1966

Mazzei, F., D'Alessandro, A., Lucarelli, F., Nava, S., Prati, P., Valli, G., Vecchi, R.: Characterization of particulate matter sources in an urban environment, Sc. Tot. Env., 401, 81-89, 2008.

Meloni, D., di Sarra, A., Herman, J. R., Monteleone, F. and Piacentino, S.: Comparison of ground-based and TOMS erythemal UV doses at the island of Lampedusa in the period 1998-2003: Role of tropospheric aerosols, J. Geophys. Res., 110, D01202, doi: 10.1029/2004JD005283, 2005.

Metzger, S., Mihalopoulos, N., and Lelieveld, J.: Importance of mineral cations and organics in gas-aerosol partitioning of reactive nitrogen compounds: case study based on MINOS results, Atmos. Chem. Phys., 6, 2549–2567, 2006.

Mihalopoulos N., Stephanou, E., Kanakidou, M. and Pilitsidis, S.: Atmospheric aerosol composition above the Eastern Mediterranean region, Tellus. 49B, 314-326, 1997.

Moreno, T., Karanasiou, A., Amato, F., Lucarelli, F., Nava, S., Calzolai, G., Chiari, M., Coz, E., Artíñano, B., Lumbreras, J., Borge, R., Boldo, E., Linares, C., Alastuey, A., Querol, X. and Gibbons, W.: Daily and hourly sourcing of metallic and mineral dust in urban air contaminated by traffic and coal-burning emissions, Atm. Env. 68, 33-44, 2013.

Nava, S., Becagli, S., Calzolai, G., Chiari, M., Lucarelli, F., Prati, P., Traversi, R., Udisti, R., Valli, G. and Vecchi, R.: Saharan dust impact in central Italy: An overview on three years elemental data records, Atm. Env., 60, 444-452, 2012.

Nava, S., Lucarelli, F., Amato, F., Becagli, S., Calzolai, G., Chiari, M., Giannoni, M., Traversi, R. and Udisti R.: Biomass burning contributions estimated by synergistic coupling of daily and hourly aerosol composition records, Science of The Total Environment, 511, 11-20, 2015.

Norris, G. A., Vedantham, R., Wade, K., Zhan, P., Brown, S., Paatero, P., Eberly, S. I. and Foley, C.: Guidance Document for PMF Applications with the Multilinear Engine. U.S.

Environmental Protection Agency, Washington, DC, EPA/600/R-09/032 (NTIS PB2009-107895), 2009

Paatero, P.: Least squares formulation of robust non-negative factor analysis, Chemometrics and Intelligent Laboratory Systems, 37, 23-35, 1997.

Paatero, P. and Hopke, P.K.: Discarding or downweighting high-noise variables in factor analytic models, Analytica Chimica Acta, 490, 277–289, 2003.

Paatero, P., Eberly, S., Brown, S. G. and Norris, G. A.: Methods for estimating uncertainty in factor analytic solutions, Atmos. Meas. Tech., 7, 781-797, 2014

Pace, G., Meloni, D. and di Sarra, A.: Forest fire aerosol over the Mediterranean basin during summer 2003, J. Geophys. Res., 110, D21202, doi:10.1029/2005JD005986, 2005.

Pace, G., di Sarra, A., Meloni, D., Piacentino, S. and Chamard, P.: Aerosol optical properties at Lampedusa (Cen- tral Mediterranean). 1. Influence of transport and identification of different aerosol types, Atmos. Chem. Phys., 6, 697–713, 2006.

Pandolfi, M., Gonzalez-Castanedo, Y., Alastuey, A., da la Rosa, J.D., Mantilla, E., de la Campa, A.S., Querol, X., Pey, J., Amato, F. and Moreno, T.: Source apportionment of PM10 and PM2.5 at multiple sites in the strait of Gibraltar by PMF: impact of shipping emissions, Environ. Sci. Pollut. Res,18, 260–269, 2011.

Pey, J., Querol, X., and Alastuey, A.: Variations of levels and composition of PM10 and PM2.5 at an insular site in the Western Mediterranean, Atmos. Res., 94, 285–299, 2009.

Pey, J., Querol, X., Alastuey, A., Forastiere, F. and Stafoggia, M.: African dust outbreaks over the Mediterranean Basin during 2001–2011: PM10 concentrations, phenomenology and trends, and Biogeosciences its relation with synoptic and mesoscale meteorology, Atmos. Chem. Phys., 13, 1395–1410, 2013.

Piazzalunga, A., Bernardoni, V., Fermo, P., Valli, G. and Vecchi, R.: Technical Note: On the effect of water-soluble compounds removal on EC quantification by TOT analysis in urban aerosol samples, Atm. Chem. and Phys. 11, 10193-10203, 2011.

Plinis, C., Charalampidis, P. E., Mihalopoulos, N., Pandis, S. N.: Contribution of particulate water to the measured aerosol optical properties of aged aerosol, Atm. Env., 82, 144-153, 2014.

Polissar, A. V., Hopke, P. K., Paatero, P., Malm, W. C. and Sisler, J. F.: Atmospheric aerosol over Alaska – 2. Elemental composition and sources, J. Geophys. Res. 103, 19045-19057, 1998.

Querol, X., Alastuey, A., Pey, J., Cusack, N. Pérez, N., Mihalopoulos, N., Theodosi, C., Gerasopoulos, E., Kubilay, N. and Koçak, M.: Variability in regional background aerosols within the Mediterranean, Atmos. Chem. Phys., 9, 4575–4591, 2009.

Randerson, J. T., Chen, Y., van der Werf, G. R., Rogers, B. M. and Morton, D. C.: Global burned area and biomass burning emissions from small fires, J. Geophys. Res., 117, G04012, doi:10.1029/2012JG002128, 2012.

Rodríguez, S., Alastuey, A., Alonso-Pérez, S., Querol, X., Cuevas, E., Abreu-Afonso, J., Viana, M., Pérez, N., Pandolfi, M. and de la Rosa, J.: Transport of desert dust mixed with North African industrial pollutants in the subtropical Saharan Air Layer, Atmos. Chem. Phys., 11, 6663–6685, 2011.

Salvador, P., Alonso-Pérez, S., Pey, J., Artíñano, B., de Bustos, J. J., Alastuey, A., and Querol, X.: African dust outbreaks over the western Mediterranean Basin: 11-year characterization of atmospheric circulation patterns and dust source areas, Atmos. Chem. Phys., 14, 6759–6775, 2014.

Schembari, C., Bove, M. C., Cuccia, E., Cavalli, F., Hjorth, J., Massabò, D., Nava, S., Udisti, R. and Prati, P.: Source apportionment of PM10 in the Western Mediterranean based on observations from a cruise ship, Atm. Env., 98, 510-518, 2014.

Seinfeld, J.H. and Pandis, S.N.: Atmospheric Chemistry and Physics: From Air Pollution to Climate Change (J. Wiley & Sons, New York, USA, Inc, 1998).

Tesche, M., Gross, S., Ansmann, A., Müller, D., Althausen, D., Fredenthaler, V. and Esselborn, M.: Profiling of Saharan dust and biomass-burning smoke with multiwavelength polarization Raman lidar at Cape Verde, Tellus, 63B, 649–676, 2011.

Traversi, R., Becagli, S., Calzolai, G., Chiari, M., Giannoni, M., Lucarelli, F., Nava, S., Rugi, F., Severi, M. and Udisti, R.: A comparison between PIXE and ICP-AES measurements of metals in aerosol particulate collected in urban and marine sites in Italy, Nucl. Instr. and Meth. B, 318, 130-134, 2014.

Turpin, B.J. and Lim, H.J: Species Contributions to PM2.5 Mass Concentrations: Revisiting Common Assumptions for Estimating Organic Mass, Aerosol Sci. Technol., 35, 602-610, 2001.

Vecchi, R., Chiari, M., D'Alessandro, A., Fermo, P., Lucarelli, F., Mazzei, F., Nava, S., Piazzalunga, A., Prati, P., Silvani, F. and Valli, G.: A mass closure and PMF source apportionment study on the sub-micron sized aerosol fraction at urban sites in Italy, Atm. Env., 42, 2240-2253, 2008.

Viana, M., Amato, F., Alastuey, A., Querol, X., Moreno, T., García Dos Santos, S., Herce, M. D. and Fernández-Patier, R.: Chemical tracers of particulate emissions from commercial shipping, Environ. Sci. Technol., 43, 7472-7477, 2009.

Wang, Y., Zhuang, G., Chen, S., An, Z. and Zheng, A.: Characteristics and sources of formic, acetic and oxalic acids in PM2.5 and PM10 aerosols in Beijing, China, Atmospheric Research, 84, 169-181, 2007.

TABLES

	Year		Winter (DJF)		Spring (MAM)		Summer (JJA)		Autumn (SON)	
n	562		136		156		142		128	
	ng/m^3		ng/m^3		ng/m^3		ng/m^3		ng/m^3	
	Av	Sd	Av	Sd	Av	Sd	Av	Sd	Av	Sd
Na	3137	1996	3584	1972	3293	1937	2953	2108	2686	1860
Mg	374	187	377	171	405	201	345	190	367	177
Al	360	549	234	432	347	570	339	446	530	682
Si	896	1389	581	1106	889	1435	830	1097	1308	1756
S	1534	806	1051	387	1644	762	2098	904	1281	634
Cl	4708	3725	5727	3945	5263	3783	3592	3663	4212	3052
K	314	223	267	190	319	238	324	198	346	256
Ca	862	1120	694	916	922	1277	761	964	1077	1237
Ti	30	46	20	35	30	49	29	41	41	56
V	5.2	5.4	2.8	3.0	6.1	5.6	8.4	6.5	3.2	3.3
Mn	5.3	7.1	3.5	5.5	5.7	7.7	5.5	6.1	6.5	8.4
Fe	304	445	200	333	316	471	290	379	415	547
Ni	2.0	1.7	1.2	1.0	2.4	1.9	3.1	1.9	1.3	1.0
Cu	1.8	1.3	1.3	1.4	1.7	1.3	2.5	1.2	1.5	1.1
Br	15	11	20	13	15	10	13	11	12	9
Sr	7	8	6	5	8	10	6	7	7	8
Na^+	3191	2191	3481	2230	3629	2352	2912	2211	2670	1751
NH_4^+	673	452	477	313	757	481	954	441	463	340
K^+	161	88	153	84	172	82	183	103	131	69
Ca^{2+}	615	717	475	433	670	859	532	508	784	905
Cl^-	4304	3743	5111	3807	4924	4019	3278	3646	3829	3072
NO_3^-	2128	1148	1866	958	2434	1232	2283	1218	1861	1028
SO_4^{2-}	3652	2074	2478	1110	4011	2059	4961	2276	3010	1674
Ossal.	144	85	101	58	151	83	194	80	126	88
Glyc.	6	5	5	4	8	6	7	6	6	4
MSA	22	23	4	4	22	19	46	25	14	14
V_{sol}	4.0	4.3	2.1	1.7	4.1	4.2	7.4	5.6	2.3	1.7
Mn_{sol}	3.1	3.9	1.9	3.9	3.3	4.2	3.4	3.0	3.9	4.2
Ni_{sol}	1.4	1.5	0.7	0.5	1.6	1.6	2.5	1.8	0.8	0.6
Cu_{sol}	1.2	1.1	0.7	1.1	1.3	1.3	1.8	0.9	0.9	0.8
As_{sol}	0.1	0.1	0.1	0.1	0.2	0.2	0.2	0.1	0.1	0.1
Pb_{sol}	2.9	2.9	2.3	2.9	3.5	2.4	3.4	2.5	2.5	3.4
	µg/m^3		µg/m^3		µg/m^3		µg/m^3		µg/m^3	
Dust	5.8	8.2	4.0	6.5	5.8	8.8	5.3	6.8	8.1	10.1
SeaS.	8.3	6.8	9.6	7.1	9.6	7.2	7.0	6.8	6.9	5.4

Table 1 – Average concentrations (Av) and standard deviation (Sd) of the main measured elements/species for all the sampling period and in the different seasons.

Ratio	Mg/Na^+	SO_4/Na^+	Cl^-/Na^+	K/Na^+	Ca/Na^+	Br/Na^+
PMF profile	0.13	0.23	1.68	0.04	0.05	0.005
Henderson and Henderson 2009	0.119	0.253	1.796	0.037	0.038	0.006

Table 2 – Elemental ratios for the sea-salt source.

EF(Mg)	EF(Si)	EF(K)	EF(Ca)	EF(Ti)	EF(Mn)	EF(Fe)	EF(Sr)
0.90	0.83	0.92	2.81	1.21	0.79	1.05	1.72

Table 3 – Enrichment factors for the mineral dust source.

FIGURE CAPTION

Figure 1 – Sampling site location.

Figure 2 – Daily and monthly mean PM_{10} concentrations in the years 2007-2008.

Figure 3 – Profiles (fraction of the elemental mass concentration, blue columns) and explained variations (red squares, referring to the right y-axis) of the identified PM_{10} sources.

Figure 4 – Temporal evolution of the PM_{10} contributions from the identified sources.

Figure 5- HYSPLIT backward trajectories ending at Lampedusa at 50 m a.s.l. corresponding to the peaks in the PM_{10} contributions due to mineral dust source (see text for the details).

Figure 6 – Temporal evolution of the “combustion emissions” and “mineral dust” sources; examples of trajectories from fires are evidenced in red, together with an example of advection from the Saharan region (green).

Figure 7 – Comparison between EC and OC data and PMF estimates of the contributions of combustion emissions and primary particulate ship emissions in the period of EC/OC data availability. Results for EC and OC are reported with solid lines, black and red, respectively, referring to the secondary axis (empty rounds report the single sample result attributing it to the central sampling day).

Figure 8 – Seasonal relative contributions to PM_{10} concentration (average over the years 2007-2008). Factors may sum to more than 100% due to number rounding.

Figure 9 – Seasonal absolute contributions to PM_{10} concentration (average over the years 2007-2008).

Figure 10 – Relative annual contributions to the PM_{10} concentration (average over the years 2007-2008).

Figure 11 – Correlation plot between the contributions from secondary sulphate and from primary particulate emitted by ships as obtained by the PMF analysis.

Figure 1

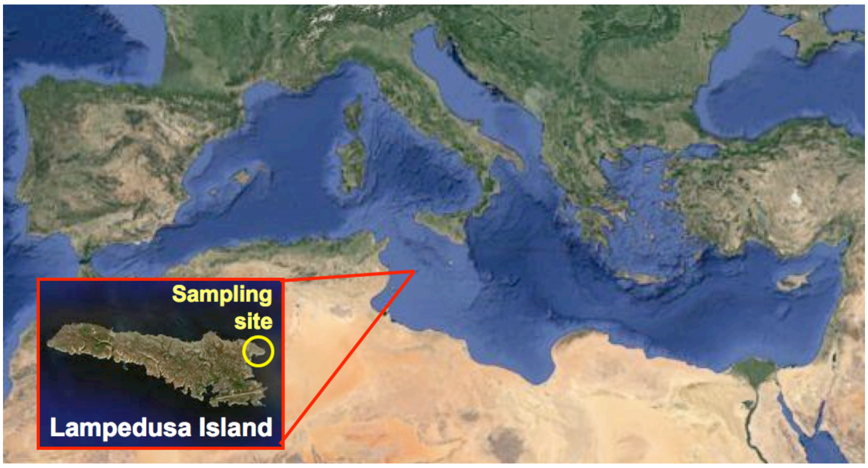

Figure 2

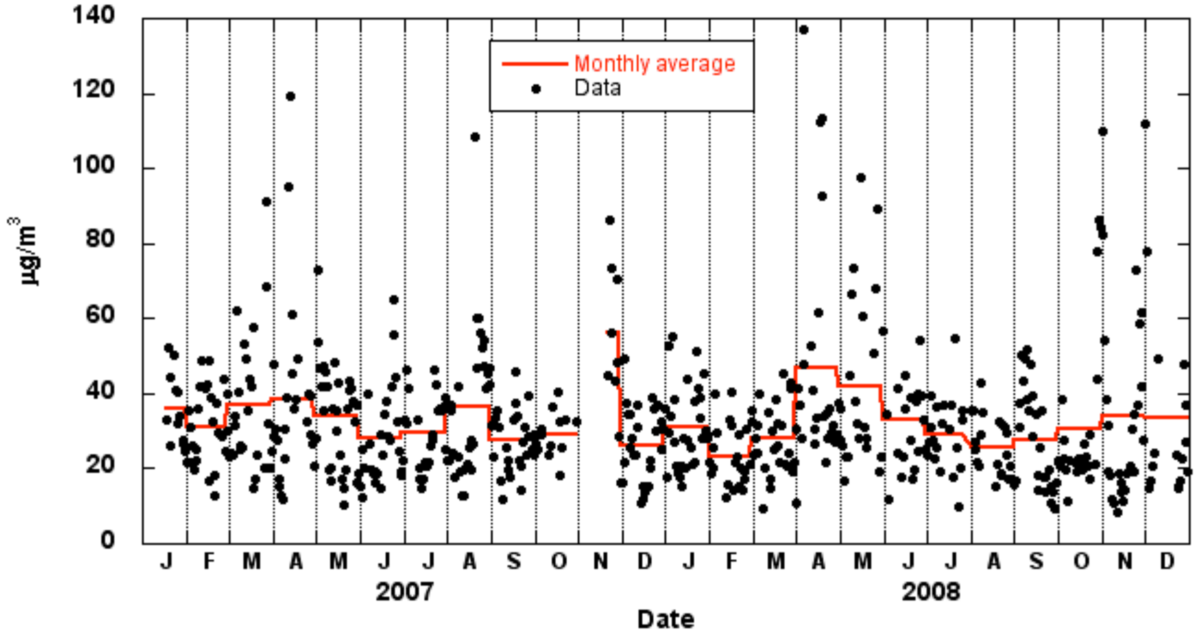

Monthly average
Data
140
120
100
80
60
40
20
0
µg/m^3
J
F
M
A
M
J
J
A
S
O
N
D
J
F
M
A
M
J
J
A
S
O
N
D
2007
2008
Date

1 Figure 3

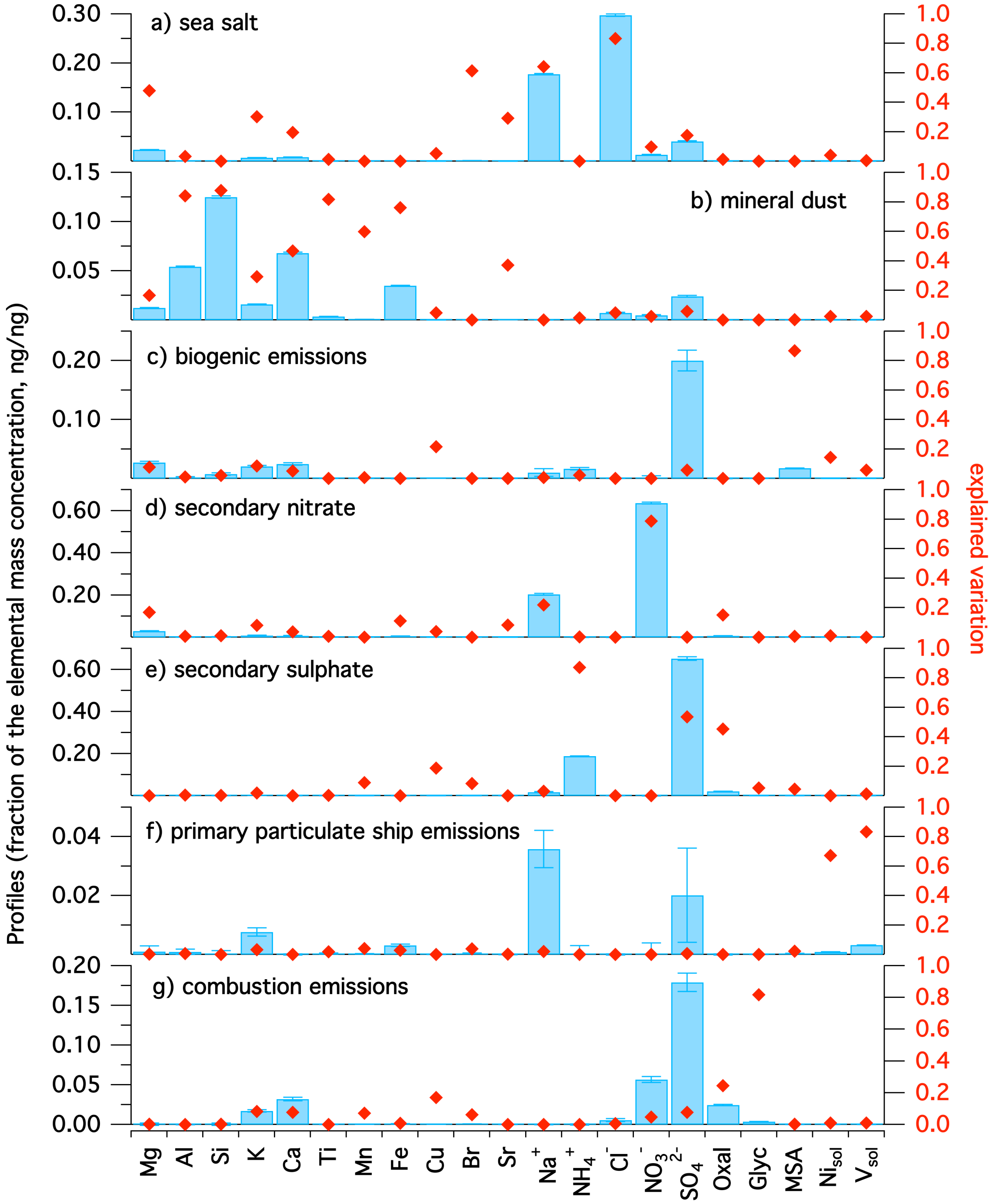
a) sea salt
b) mineral dust
c) biogenic emissions
d) secondary nitrate
e) secondary sulphate
f) primary particulate ship emissions
g) combustion emissions
Profiles (fraction of the elemental mass concentration, ng/ng)
explained variation
0.30
0.20
0.10
0.15
0.05
0.60
0.40
0.04
0.02
0.00
1.0
0.8
0.6
0.4
0.2
0.0
Mg
Al
Si
K
Ca
Ti
Mn
Fe
Cu
Br
Sr
Na$^+$
NH$_4^+$
Cl$^-$
NO$_3^-$
SO$_4^{2-}$
Oxal
Glyc
MSA
Ni$_{sol}$
V$_{sol}$

2

3

1 Figure 4


2007
2008
J F M A M J J A S O N D J F M A M J J A S O N D
a) sea salt
60
40
20
0
b) mineral dust
120
80
40
0
c) biogenic emissions
10
8
6
4
2
0
d) secondary nitrate
12
8
4
0
e) secondary sulphate
16
12
8
4
0
f) primary ship emissions
10
8
6
4
2
0
g) combustion emissions
10
8
6
4
2
0
PM$_{10}$ contribution (µg/m^3)

2

Figure 5

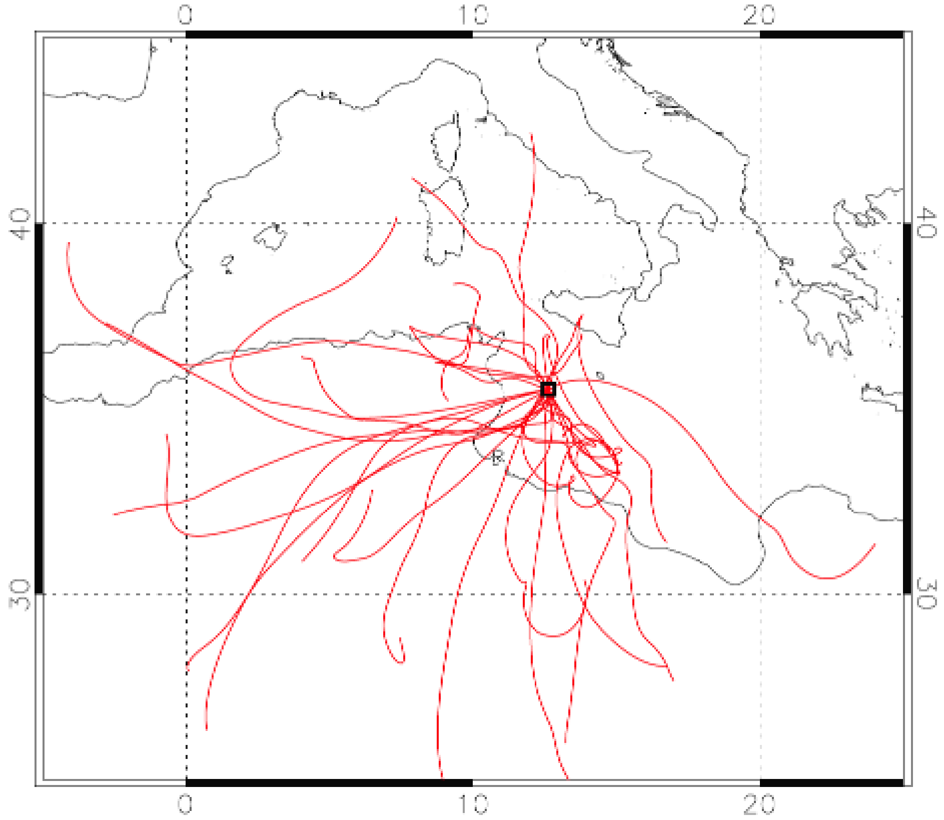

Figure 6

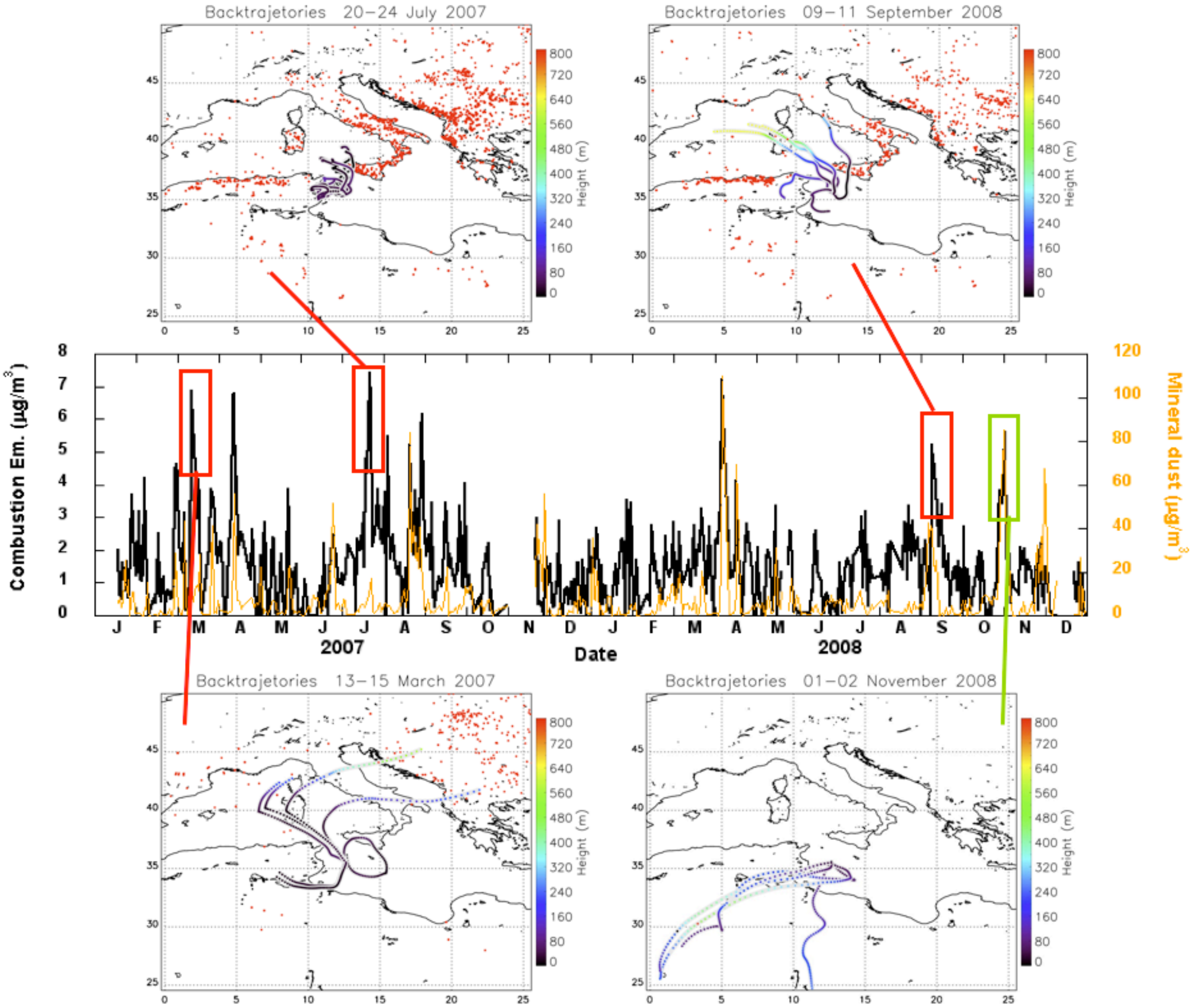
Backtrajetories 20–24 July 2007
Backtrajetories 09–11 September 2008
Backtrajetories 13–15 March 2007
Backtrajetories 01–02 November 2008
Height (m)
800
720
640
560
480
400
320
240
160
80
0
45
40
35
30
25
0
5
10
15
20
25
Combustion Em. (µg/m³)
Mineral dust (µg/m³)
8
7
6
5
4
3
2
1
0
120
100
80
60
40
20
0
J F M A M J J A S O N D J F M A M J J A S O N D
2007
2008
Date

Figure 7

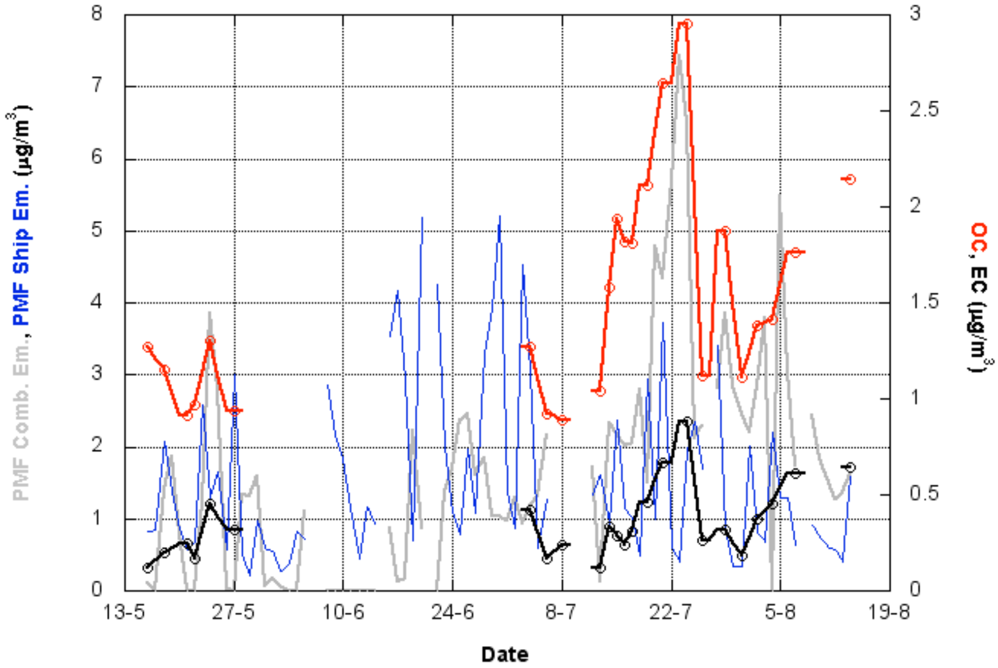

8
7
6
5
4
3
2
1
0
PMF Comb. Em., PMF Ship Em. ($\mu g/m^3$)
3
2.5
2
1.5
1
0.5
0
OC, EC ($\mu g/m^3$)
13-5
27-5
10-6
24-6
8-7
22-7
5-8
19-8
Date

Figure 8

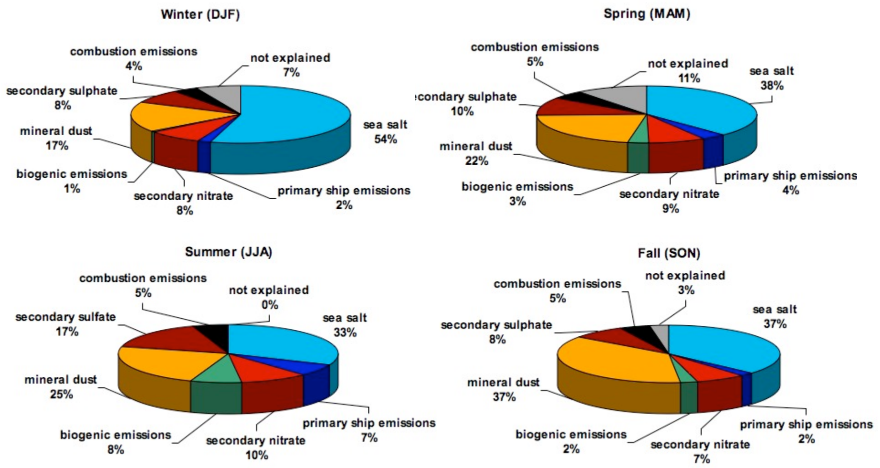
Winter (DJF)
combustion emissions 4%
not explained 7%
secondary sulphate 8%
mineral dust 17%
sea salt 54%
biogenic emissions 1%
secondary nitrate 8%
primary ship emissions 2%
Spring (MAM)
combustion emissions 5%
not explained 11%
sea salt 38%
econdary sulphate 10%
mineral dust 22%
biogenic emissions 3%
secondary nitrate 9%
primary ship emissions 4%
Summer (JJA)
combustion emissions 5%
not explained 0%
secondary sulfate 17%
sea salt 33%
mineral dust 25%
biogenic emissions 8%
secondary nitrate 10%
primary ship emissions 7%
Fall (SON)
combustion emissions 5%
not explained 3%
secondary sulphate 8%
sea salt 37%
mineral dust 37%
biogenic emissions 2%
secondary nitrate 7%
primary ship emissions 2%

Figure 9

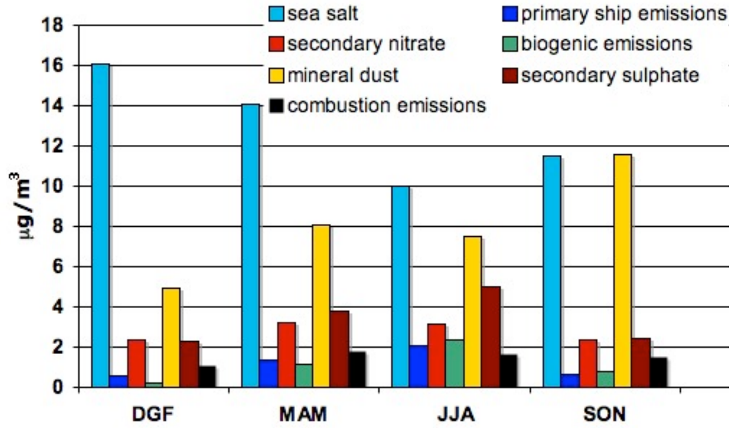
sea salt
primary ship emissions
secondary nitrate
biogenic emissions
mineral dust
secondary sulphate
combustion emissions
μg/m3
18
16
14
12
10
8
6
4
2
0
DGF
MAM
JJA
SON

Figure 10

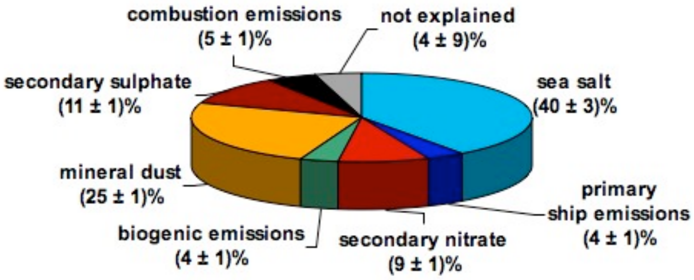
combustion emissions
(5 ± 1)%
not explained
(4 ± 9)%
secondary sulphate
(11 ± 1)%
sea salt
(40 ± 3)%
mineral dust
(25 ± 1)%
primary
ship emissions
(4 ± 1)%
biogenic emissions
(4 ± 1)%
secondary nitrate
(9 ± 1)%

Figure 11

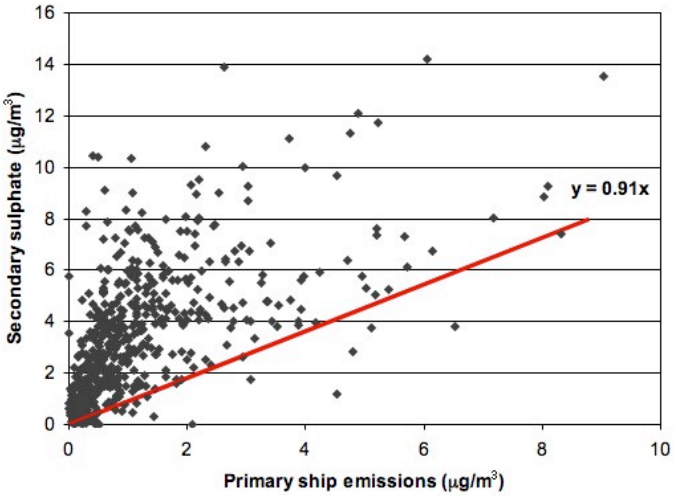
Secondary sulphate (μg/m^3)
Primary ship emissions (μg/m^3)
y = 0.91x
0
2
4
6
8
10
12
14
16
0
2
4
6
8
10